J. Phys. D: Appl. Phys. **41** (2008) 000000 (7pp) doi:10.1088/0022-3727/41/1/000000

Er^{3+} and Yb^{3+} concentration effect in the spectroscopic properties and energy transfer in Yb^{3+}/Er^{3+} codoped tellurite glasses

H Desirena[1], E De la Rosa[1,3], A Shulzgen[2], S Shabet[2] and N Peyghambarian[2]

[1] Centro de Investigaciones en Optica, A. P. 1-948, León Gto. 37160, México
[2] College of Optical Science, University of Arizona, Tucson, AZ 85721, USA

E-mail: elder@cio.mx and hagdes@cio.mx

Received 12 January 2008, in final form 15 February 2008
Published
Online at stacks.iop.org/JPhysD/41

Abstract

Spectroscopic properties of Yb^{3+}/Er^{3+} codoped tellurite glasses as a function of Er^{3+} and Yb^{3+} concentration have been investigated. Under 970 nm excitation three strong up-conversion emission bands centred at 525, 546 and 656 nm were observed, and the characteristic near infrared emission band was centred at 1.53 μm. With fluorescence and radiative lifetime the quantum efficiency (QE) of infrared (1.53 μm) and visible upconversion (546 and 660 nm) emissions was calculated. The maximum stimulated emission cross section for $^4I_{13/2} \rightarrow {}^4I_{15/2}$ transition of Er^{3+} is 9.7×10^{-20} cm^2 for 3/0.5 mol%. The energy transfer (ET) efficiency from Yb^{3+} to Er^{3+} $(^4F_{5/2}) + (^4I_{15/2}) \rightarrow (^4F_{7/2}) + (^4I_{13/2})$ was calculated, being the maximum ET of 69% for 0.5 mol% of Er^{3+} with 4.5 mol% of Yb^{3+}. The results indicate that both ET and QE depend mostly on Er^{3+} rather than on Yb^{3+} concentration.

AQ1 (Some figures in this article are in colour only in the electronic version)

1. Introduction

Among numerous rare earth doped glasses, Er^{3+} doped tellurite is one of the systems that have attracted considerable interest due to its use as a fibre amplifier for broadband amplification at 1.53 μm [1, 2] and frequency upconversion to obtain efficient visible laser emission [3]. A broadband larger than 60 nm, AQ2 larger than that obtained in phosphate glasses, has been reported for 1.53 μm emission band, the strong upconversion emission being the main drawback that could be useful for other purposes. Recently, several works on tellurite glasses have been reported by different authors. There, mainly the effect of Er^{3+} concentration on the spectroscopic and optical properties has been studied [4–11]. However, only a few experimental works on the spectroscopic properties in Er^{3+}/Yb^{3+} codoped tellurite glasses have been reported [12–14]. Yb^{3+} ions ars used as sensitizers to enhance the pumping efficiency of 980 nm laser diode (LD) emission, since Yb^{3+} exhibits a large absorption cross section and a broad absorption band between 850 and 1080 nm compared with weak absorption of Er^{3+} ions [15]. In this system, Yb^{3+} absorbs the radiation at 980 nm and transfers the energy to Er^{3+} (acceptor) according to the equation $Yb^{3+}(^2F_{5/2}) + Er^{3+}(^4I_{15/2}) \rightarrow Yb^{3+}(^2F_{7/2}) + Er^{3+}(^4I_{11/2})$. The overall result is the increment of population in the level $^4I_{13/2}$ of Er^{3+}; as a consequence the luminescence intensity is stronger after relaxation to the ground state. It is well known that the dynamics of Er^{3+} emission depends on both Er^{3+} and Yb^{3+} concentrations and are strongly influenced by the optical properties of the host. Thus, it is convenient to understand such a mechanism to optimize any specific emission, either visible or near infrared (NIR) emission. To the best of our knowledge, there is no detailed study on the effect of Er^{3+} and Yb^{3+} concentrations on the spectroscopic properties and

[3] Author to whom any correspondence should be addressed.

 © 2008 IOP Publishing Ltd Printed in the UK

JNL: JPD PIPS: 270490 TYPE: PAP TS: NEWGEN DATE: 5/3/2008 EDITOR: MM

energy transfer (ET) efficiency in Er^{3+}/Yb^{3+} codoped tellurite glasses.

The optical, mechanical and chemical properties of the host depend on its composition. Then, the selection of the glass components is very important in the development of high performance tellurite glass. The glass former is TeO_2 and several glass network modifiers have been used. Alkalis are well-known modifiers widely used in phosphate glasses where spectroscopic, thermo-mechanical and physical properties have been modified [16–18]. Because of the ion size and electronic properties, each ion modifies the glass properties in a different way. Wang *et al* reported that TeO_2–ZnO–Na_2O glass is a good candidate for feasible rare earth doped fibre amplifiers [19]. The addition of Na_2O improves the solubility of rare earth leading to the possibility of using a high concentration of dopants, which is very important in the design of high efficiency short length fibre amplifiers. However, others alkalis, such as Cs_2O, Rb_2O, K_2O and Li_2O, could improve the optic, spectroscopic and physical properties of the glass. Recently, we have systematically studied the effect of other alkalis and it was found that the use of Li_2O in the system TeO_2–ZnO–R_2O–La_2O_3 produced the highest refractive index, the highest glass transition temperature, the widest range of transmission, the lowest thermal expansion coefficient, the lowest OH content, the highest chemical durability and the highest density. The complete study on the effect of alkalis in the properties of tellurite glasses is presented elsewhere [20].

In this investigation, Er^{3+}/Yb^{3+} codoped tellurite glasses with a composition of TeO_2–ZnO–Li_2O–La_2O_3 were prepared and the spectroscopic properties were studied in detail. In particular, in this study we focus on analysing the dependence of ET in Er^{3+} and Yb^{3+} concentrations. The Judd–Ofelt (J–O) intensity parameters and quantum efficiency (QE) were calculated. The emission intensity of both infrared and upconverted signals was investigated and the physical mechanisms were explained in terms of the energy transfer and cross-relaxation process.

2. Experimental

The glass composition was $70TeO_2$–$20ZnO$–$5Li_2O$–$(5-x-y)La_2O_3$–xEr_2O_3–yYb_2O_3(mol%), where $x = 0.10$, 0.15, 0.30, 0.5, 0.75 at $y = 0.5$ and $y = 1$, 2, 3, 4.5 at $x = 0.5$. All samples were prepared from the starting chemical constituent tellurite oxide (TeO_2), zinc oxide (ZnO), lithium carbonate (Li_2CO_3), erbium oxide (Er_2O_3), ytterbium oxide (Yb_2O_3) and lanthanum oxide (La_2O_3). All reactants were analytical grade and used as received. The calculated quantities of the chemicals were mixed in an agate mortar and melted in a PDI electric furnace at 900 °C for 1 h in platinum crucibles so that a homogeneously mixed melt was obtained. The melt was cast into a suitable brass mould kept at 300 °C and pressed by a similar brass plate. The obtained glasses were subsequently annealed at temperatures from 300 to 380 °C depending on the glass composition. The time to finish the annealing process took around 18 h. The samples were then polished to optical quality and only bubble- and streak-free samples were taken for optical measurements. The density of each sample was measured by the Archimedes method using water distilled as the immersion liquid. Samples were cut and then polished to 2 mm thick slabs for different measurements. The transmission spectra were measured using a UV-VIS-NIR spectrophotometer (Perking Elmer) in the range 300–1800 nm. The refractive index of the samples was measured at 632.8, 800 and 1550 nm by the prism coupler technique (Metricon, Model 2010). The emission spectra were recorded by exciting the samples at 970 nm with a low power AlGaAs LD. The signal emitted was focused onto a SP-2357 monochromator (Acton Research) and detected by a thermoelectrically cooled InGaAs detector (Judson) and a photomultiplier tube R955 (Hamamatsu). The signal detected was processed in a PC. The decay profile corresponding to 1.53 μm was recorded using a SR540 chopper (Stanford Research System) at 15 Hz and connecting the photodetector directly to an oscilloscope (LT344 LeCroy). All the optical measurements were performed at room temperature.

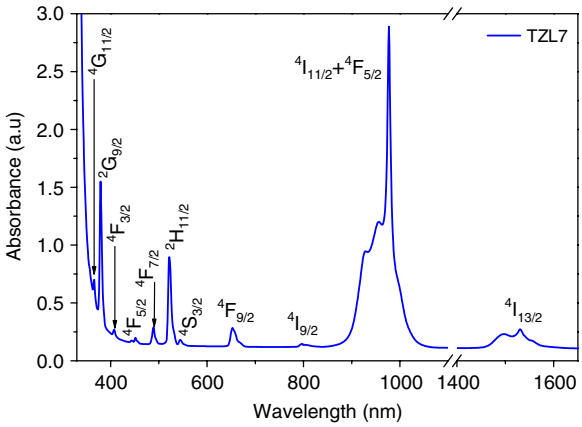

Figure 1. Absorption spectrum of Er^{3+}/Yb^{3+} codoped tellurite glass.

3. Results and discussion

3.1. J–O parameters

From the absorption spectrum of Er^{3+}/Yb^{3+} codoped tellurite glasses, nine bands were considered to predict the J–O parameter, see figure 1. The calculated line strength for the dipole transition between J and J' is obtained by the theoretical expression derived by Judd [21] and Ofelt [22]:

$$S_{\mathrm{calc}}(J \rightarrow J') = \sum_{t=2,4,6} \Omega_t |\langle (S, L)J||U^{(t)}||S', L')J'\rangle|^2. \quad (1)$$

Here U^t are the doubly reduced matrix elements of the unit tensor operator of rank $t = 2$, 4 and 6, which are calculated from the intermediate coupling approximation. The reduced matrix elements are virtually independent of the ligand species surrounding the rare earth (RE^{3+}) ions and thus approximately unchanged from host to host. Ω_2, Ω_4 and Ω_6 are the phenomenological J–O parameters which exhibit the influence of the host. The complete procedure of obtaining the J–O parameters and some spectroscopic properties in tellurite glasses has been described elsewhere [5]. The values of such parameters and the root mean square deviation for Er^{3+}/Yb^{3+} codoped tellurite glasses under study

Table 1. J–O parameters for various tellurite glass compositions.

Glass composition	Ω_2 (10^{-20} cm^2)	Ω_4 (10^{-20} cm^2)	Ω_6 (10^{-20} cm^2)
TeO_2–Nb_2O_5–Na_2O[a]	6.86	1.53	1.12
TeO_2–ZnO–Na_2O[b]	5.98	1.32	1.47
TeO_2–WO_3–Bi_2O_3[c]	6.06	1.57	0.95
TeO_2–ZnO–K_2O[d]	5.95	2.06	1.07
TeO_2–ZnO–Li_2O[e]	6.56	1.60	1.44

[a] [7].
[b] [5].
[c] [23].
[d] [24].
[e] Reported in this paper.

are $\Omega_2 = 6.56 \times 10^{-20}$ cm^2, $\Omega_4 = 1.60 \times 10^{-20}$ cm^2 and $\Omega_6 = 1.44 \times 10^{-20}$ cm^2 with RMS $= 0.142 \times 10^{-20}$ cm^2. The calculated values were performed with an error of $\pm 10\%$. The obtained J–O parameters follow the typical behaviour $\Omega_2 > \Omega_4 > \Omega_6$ reported for tellurite glasses and are in agreement with the results reported recently for various glass compositions, as shown in table 1. Once the J–O parameters are known, several spectroscopic properties can be calculated, such as the radiative decay rates, branching ratios and spectroscopy quality factor (χ); this last parameter was found to be 1.11 and is in agreement with the results reported by other authors [7, 10]. From radiative decay rates the radiative lifetimes were calculated and the values are 3.79 ms, 308 μs and 252 μs for $^4I_{13/2}$, $^4F_{9/2}$ and $^4S_{3/2}$ levels, respectively.

3.2. *Absorption (σ_{abs}) and emission cross section (ECA) (σ_{emi})*

The absorption cross section of the $^4I_{13/2} \rightarrow {}^4I_{15/2}$ (1.53 μm) transition of Er^{3+} has been determined from the absorption spectrum using the relation

$$\sigma_a = \frac{2.303 \log(I_0/I)}{NL}, \tag{2}$$

where $\log(I_0/I)$ is the optical density, L is the sample thickness and N is the concentration of the Er^{3+} ion. The stimulated ECS was obtained according to McCumber theory from the expression [25]

$$\sigma_e(v) = \sigma_a(v) \exp[(\varepsilon - h(c/\lambda))/kT], \tag{3}$$

where v is the photon frequency, ε is the net free energy required to excite one erbium ion from the $^4I_{15/2}$ to the $^4I_{13/2}$ level at temperature T, h is Planck's constant, k is the Boltzmann constant and c is the light velocity in the vacuum. $\varepsilon = 6550$ cm^{-1} was estimated by using the approximation $\varepsilon = E_o + 21E_2 - 28E_1$ [26]. In this case, three basic assumptions are considered: (1) the Stark levels for a given manifold are equally spaced, $E_{ij} = (j-1)E_i$, with a degeneracy equal to 7 and 8 for $^4I_{13/2}$ and $^4I_{15/2}$, respectively; (2) E_0 is the energy between the two levels and was calculated taking the average between the absorption and the emission peaks; (3) E_1 and E_2 are calculated measuring the half width energy calculated from the wavelength peak to the point where the signal decreased to 5%. The values of both absorption and ECS as a function of Er^{3+} and Yb^{3+} concentrations are shown in figure 2. The sample with lower erbium concentration has the largest peak ECS of 1.0×10^{-20} cm^2 which then decreases with the increment in Er^{3+} content, see figure 2(*c*). With Yb^{3+} concentration, the maximum of 9.71×10^{-20} cm^2 was obtained at 3 mol% of Yb^{3+} which diminishes for higher concentration. The calculated values of stimulated ECS are in agreement with the results reported recently [7] and are higher than the values reported for silica (7.9×10^{-21} cm^2) [27] and phosphate glass (6.8×10^{-21} cm^2) [28]. The larger cross section is expected due to the large refractive index of the host induced partly by the content of Li. This relationship is also established from J–O theory.

3.3. *Fluorescence properties of Er^{3+} /Yb^{3+} codoped tellurite glass*

3.3.1. Infrared and upconversion emission. The well-known NIR emission ($^4I_{13/2} \rightarrow {}^4I_{15/2}$) of Er^{3+} in the Yb^{3+}/Er^{3+} co-doped tellurite glasses was centred at 1.53 μm with the spectral bandwidth ranging from 51 to 71 nm, depending on the concentration of both ions, as shown in figure 3(*a*). This means there is an increment of 18 nm in the bandwidth just controlling the ion concentration. The obtained results show a continuous increment of the bandwidth with the increment of both Er^{3+} and Yb^{3+} ions. Note that lower change concentrations of Er produce an almost similar bandwidth than the higher change concentration of Yb. The ion concentration also modifies the intensity of the signal increasing monotonically with the increment of Yb^{3+} and showing a maximum at 0.5 mol% of Er^{3+} ions as indicated in figure 3(*b*). Such a dependence clearly indicates the importance of the right concentration of both ions, in particular the important role of sensitizer Yb^{3+}. The concentration of both ions should be appropriate in order to minimize the upconversion emission and non-radiative processes due to cluster formation. Both phenomenona reduce the fluorescence lifetime of the $^4I_{13/2}$ level, which leads to a decrease in the laser efficiency. Although larger concentrations of sensitizer ion help in dispersing the Er ion and enhancing its excitation, it also enhances upconversion emission. This last process presents a stronger dependence at high pump powers and this effect is much more pronounced for a larger concentration of dopants. In addition, it has been demonstrated that higher concentrations of Yb induce an increment of heat that induces a deleterious effect on the laser efficiency. These results suggest the use of higher concentration of ions for amplifiers and lower concentration for laser devices [29]. In addition to the NIR signal emitted, two strong visible bands, green ($^2H_{11/2} + {}^4S_{3/2} \rightarrow {}^4I_{15/2}$) and red ($^4F_{9/2} \rightarrow {}^4I_{15/2}$), centred at 526 nm, 548 nm and 660 nm, respectively, were observed and are shown in figure 4. The visible emission is the result of the well-known upconversion process and it depends on the concentration of both Yb and Er ions. The overall intensity of the upconverted signal increases monotonically with the Yb concentration but decreases with Er being the maximum at 0.25 mol% of Er_2O_3, see figure 5(*a*). The increment is explained in terms of the ET efficiency due to

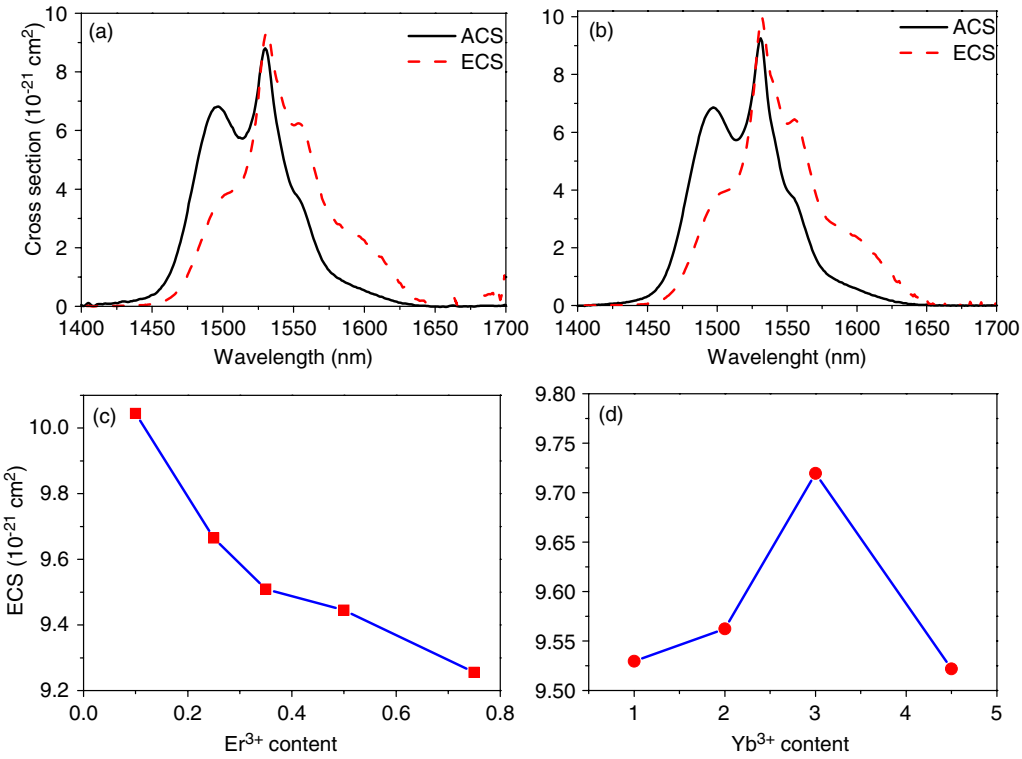

Figure 2. Absorption and ECS of Er^{3+} in Er^{3+}/Yb^{3+} codoped tellurite glass: (*a*) 0.75/0.5 mol%, (*b*) 0.5/3 mol%, (*c*) σ_e as a function of Er^{3+} concentration and (*d*) σ_e as a function of Yb^{3+} concentration.

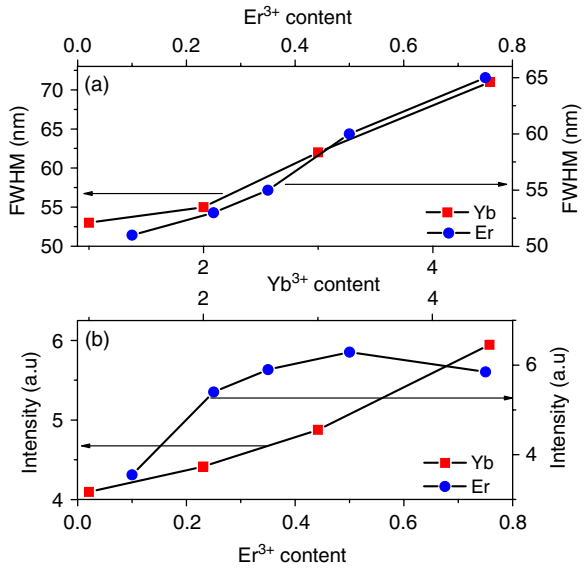

Figure 3. Emission spectra of Er at 1.53 μm in Er^{3+}/Yb^{3+} codoped tellurite glass: (*a*) FWHM behaviour as a function of Er and Yb concentration and (*b*) intensity at 1.53 μm as a function of Er and Yb concentrations.

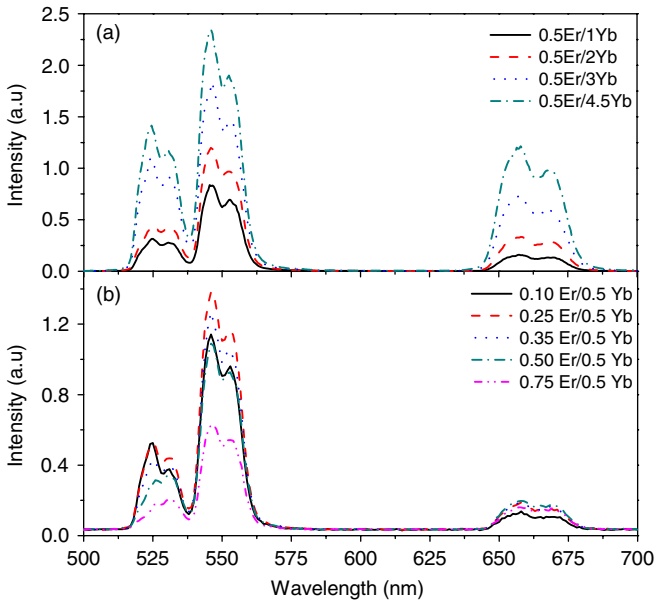

Figure 4. Upconversion emission for (*a*) Er^{3+}/Yb^{3+} (x/0.5 mol%) and (*b*) Er^{3+}/Yb^{3+} (0.5/y mol%).

the increment in donors while the decrement in signal is presumably due to the quenching effect of acceptors. Both visible bands increase but the red one increases faster as shown in figure 5(*b*), where the green/red ratio of the integrated signal is plotted. This behaviour is in agreement with other reports where the red band increases with the increase in Yb concentration. The visible emissions are relaxation pathways in contrast to the pathway associated with 1.53 μm emission, and then the enhancement of the former is deleterious to the very important emission associated with the communication window. Then, a better understanding of the dynamics of ions' interaction is very important.

The integrated upconverted (I_{upc}) signal was plotted as a function of the pumping power (I_{pp}). Experimental data

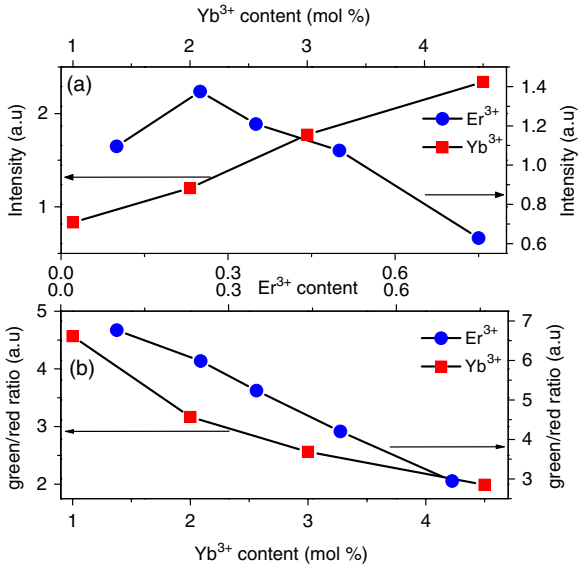

Figure 5. (*a*) Upconversion intensity of $^4S_{3/2} \rightarrow {}^4I_{15/2}$ transition and (*b*) the green/red ratio of the integrated signal.

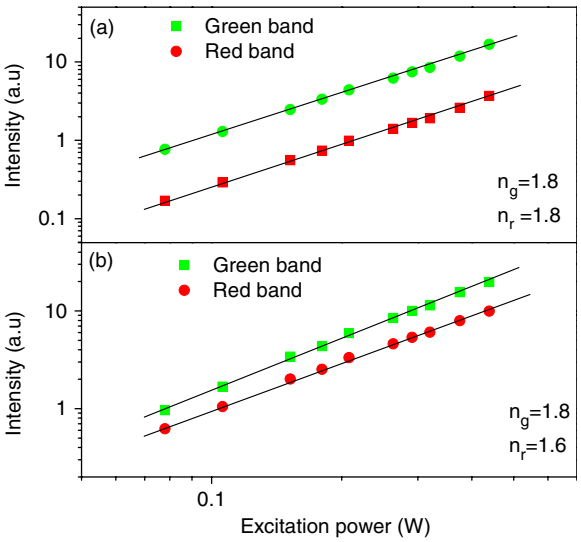

Figure 6. Pump power dependence of green and red emissions: (*a*) 0.5Er/0.5Yb mol% and (*b*) 0.5Er/4.5Yb mol%.

were fitted by the expression $I_{upc} = kI_{pp}^n$ where n denotes the number of photons involved in the process and k is the proportionality constant. Figure 6 shows such behaviour for lowest and highest concentrations of Yb^{3+} ions; in both cases $n \sim 2$ for both green and red bands. According to this, the physical mechanism describing both visible and NIR emissions is as follows. Er^{3+} ions (acceptors) are excited by the ET from Yb^{3+} (donor) that are excited directly ($^2F_{5/2} \rightarrow {}^2F_{7/2}$) by the pumping signal. In all cases the direct excitation of Er is also possible; however, ET is most probably due to the larger absorption cross section of Yb and the resonance between $^2F_{5/2} \rightarrow {}^2F_{7/2}$ and $^4I_{15/2} \rightarrow {}^4I_{11/2}$ transitions of Yb and Er, respectively, as shown in the energy diagram in figure 7. A part of the $^4I_{11/2}$ excited ions relaxes non-radiatively to the $^4I_{13/2}$ level and from there relaxes to the ground state producing the 1.532 μm emission band. And a part was promoted to $^4F_{7/2}$

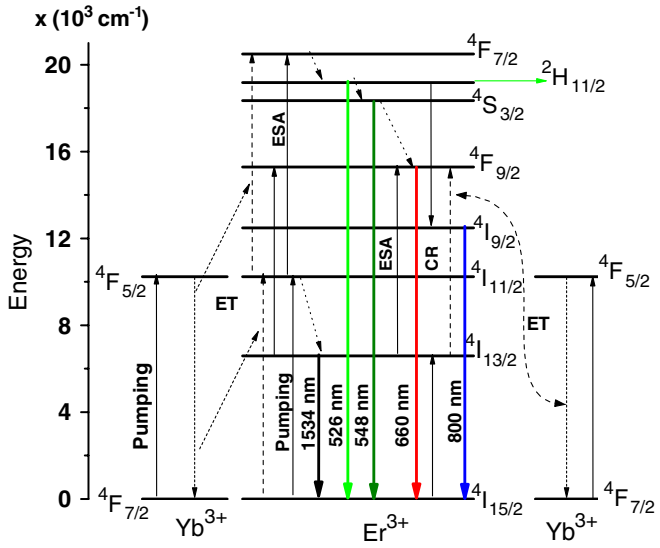

Figure 7. Energy diagram of the Er/Yb system and the mechanism proposed to explain both visible and infrared emissions.

by the ET from the relaxation of another excited Yb or Er ($^4I_{11/2} \rightarrow {}^4I_{15/2}$) ion. The $^4F_{7/2}$ level decays non-radiatively to $^2H_{11/2}$+$^4S_{3/2}$ due to phonon energy. From there the population decays to the ground state producing the green emissions centred at 526 and 548 nm. And a part decays non-radiatively to $^4F_{9/2}$ to finally decay to the ground state ($^4F_{9/2} \rightarrow {}^4I_{15/2}$) producing the red emission centred at 670 nm. This visible band is also enhanced by increasing the concentration of both donor and acceptors. In this case, a part of the population in the $^4I_{13/2}$ level is promoted to $^4F_{9/2}$ by the ET from another donor $Yb^{3+}(^2F_{5/2}) + Er^{3+}(^4I_{13/2}) \rightarrow Yb^{3+}(^2F_{7/2}) + Er^{3+}(^4F_{9/2})$. The enhancement of the red band with Er concentration is explained in terms of the increment in population of $^4I_{13/2}$ due to the cross-relaxation (CR) process $Er^{3+}(^2H_{11/2}) + Er^{3+}(^4I_{13/2}) \rightarrow Er^{3+}(^4I_{9/2}) + Er^{3+}(^4I_{13/2})$. In fact, CR phenomena also explain the low value $n = 1.6$ for the red emission band. And the enhancement with Yb is explained in terms of the ET from donors to acceptors due to the high concentration of donors, see figure 7. The mechanism proposed for explaining the signal emitted by codoped glasses is well described in figure 7.

3.3.2. Fluorescence lifetime. Experimental results suggest that the physical mechanism associated with the signal emitted does not change with the ion concentration. However, fluorescence decay time strongly depends on the ion concentration. Figure 8 shows a typical plot of decay time for three different concentrations for each signal emitted. Notice the single exponential decay at 1.53 μm for different Yb^{3+} concentrations. The fluorescence decay times of all samples under study for green (560 nm), red (670 nm) and NIR (1.532 μm) emissions are shown in table 2. The fluorescence decay time of $^4I_{13/2} \rightarrow {}^4I_{15/2}$ transition increases from 4.00 to 4.23 ms when Er_2O_3 increases from 0.10 to 0.35 mol% and then decreases to 3.69 ms for 0.75 mol%, see figure 9(*a*). The increment in the fluorescence lifetime of the $^4I_{13/2}$ level is the result of the concentration optimization of the acceptor and the decrease is the result of the fluorescence

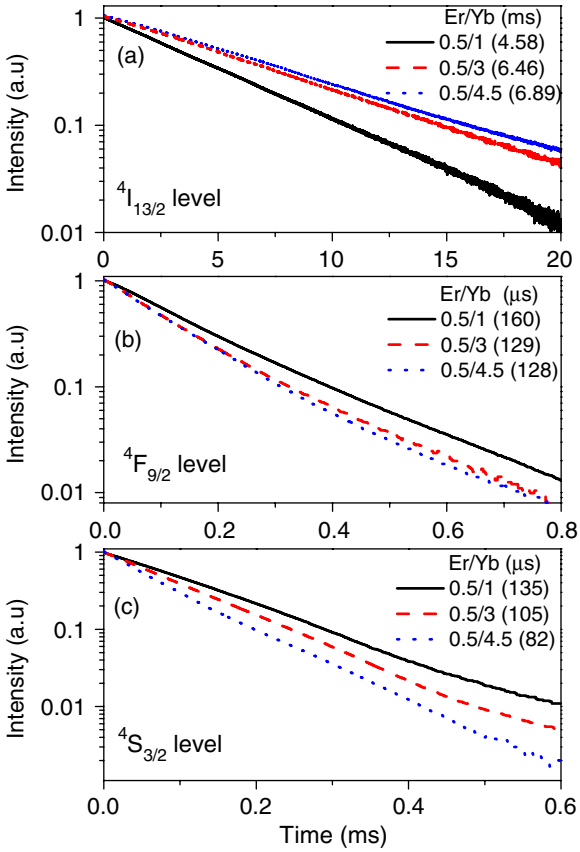

Figure 8. Fluorescence decay time for 0.5/1, 0.5/3 and 0.5/4.5 mol% of Er^{3+}/Yb^{3+} for (*a*) $^4I_{13/2} \rightarrow {}^4I_{15/2}$, (*b*) $^4F_{9/2} \rightarrow {}^4I_{15/2}$ and (*c*) $^4S_{3/2} \rightarrow {}^4I_{15/2}$ transitions.

quenching of Er^{3+} due to cluster formation provided by the higher concentration. The concentration effect is explained by differential site occupancy [30] and by the presence of the radiation trapping effect. In this phenomenon, photons spontaneously relaxed from the $^4I_{13/2}$ level are re-absorbed by the neighbouring ions in the ground state ($^4I_{15/2}$). This process of re-absorption and re-emission is repeated and the overall result is an increase in the lifetime in comparison with a single isolated ion. After optimum concentration the cluster formation occurs and, in turn, fluorescence quenching. It has been reported that such an effect is dependent on the sample size, refractive index and spectral overlap between fluorescence and absorption [31]. On the other hand, the fluorescence lifetime of such a transition increases monotonically from 4.60 to 6.90 ms when Yb_2O_3 increases from 1.0 to 4.5 mol%, see figure 9(*b*). This is partly the result of the higher concentration of sensitizer and the better excitation process of Er via the ET from Yb, as reported previously [28]. And partly it is the result of a better dispersion of Er avoiding cluster formation that in turn avoids fluorescence quenching. The ionic radius of Yb^{3+} ions is similar to that of Er^{3+} ions; as a consequence Yb^{3+} ions can act as a disperser of Er^{3+} ions reducing the cluster formation. The measured lifetime confirms that the effect of concentration quenching of the $^4I_{13/2}$ level decreases with an increase in Yb^{3+} in this glass host, as listed in table 2. The fluorescence decay times of $^4S_{3/2}$ and $^4F_{9/2}$ levels decay monotonically as a function of

Table 2. Fluorescence lifetime and QE as a function of Er^{3+} and Yb^{3+} concentrations.

Er/Yb (mol%)	Fluorescence lifetime			Quantum efficiency (%)		
	$^4S_{3/2}$ (μs)	$^4F_{9/2}$ (μs)	$^4I_{13/2}$ (ms)	$^4S_{3/2}$	$^4F_{9/2}$	$^4I_{13/2}$
0.10/0.5	160	194	4.01	63	67	100
0.25/0.5	153	163	4.21	61	55	100
0.35/0.5	138	155	4.23	55	51	100
0.50/0.5	114	132	4.02	45	42	100
0.75/0.5	80	126	3.69	31	40	96
0.5/1.0	135	160	4.58	91	56	100
0.5/2.0	111	147	4.78	76	52	100
0.5/3.0	105	129	6.46	71	46	100
0.5/4.5	82	128	6.89	55	45	100

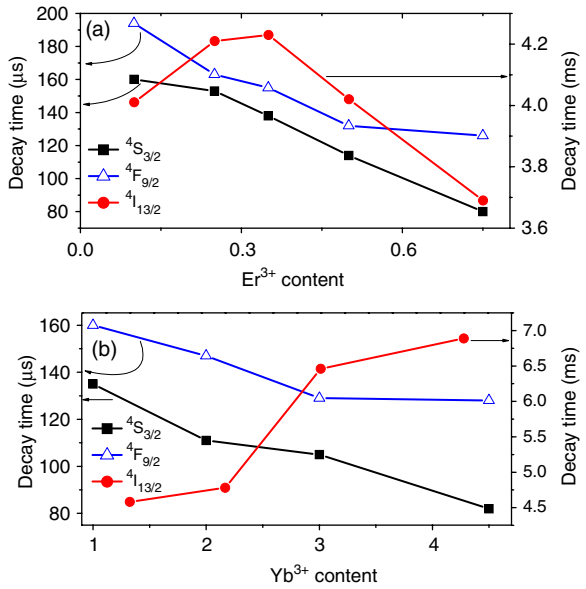

Figure 9. Fluorescence decay time of $^4S_{3/2}$, $^4F_{9/2}$ and $^4I_{13/2}$ levels as a function of (*a*) Er and (*b*) Yb concentrations.

both Er^{3+} and Yb^{3+} concentrations. For green emission it ranges from 160 μs and 135 μs to 80 μs, respectively, and for red emission it ranges from 194 μs and 160 μs to 126 μs for different concentrations of Er and Yb, respectively, as shown in figures 9(*a*) and (*b*). The lifetime for the green band diminishes faster than the red band. Notice that the lifetime decay of the red band was reduced by increasing Er and Yb concentrations. Such a behaviour confirms the presence of cross-relaxation and ET processes populating $^4F_{9/2}$, see figure 7. Comparing the measured decay time with that calculated by J–O theory, it is possible to calculate the QE for the three observed transitions. It was calculated by using the expression

$$\eta = \tau_{\text{mea}}/\tau_{\text{rad}}, \tag{4}$$

where τ_{mea} is the experimentally measured lifetime and τ_{rad} is the calculated radiative lifetime obtained from J–O parameters. The values of QE for all Yb/Er co-doped tellurite glass are listed in table 2. The QE for $^4S_{3/2} \rightarrow {}^4I_{15/2}$ and $^4F_{9/2} \rightarrow {}^4I_{15/2}$ transitions decreases with the increase in Er^{3+} and Yb^{3+} concentrations; meanwhile the $^4I_{13/2} \rightarrow {}^4I_{15/2}$ transition is 100%.

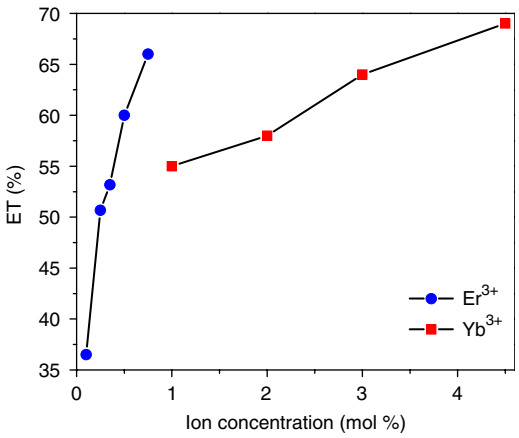

Figure 10. ET efficiency as a function of Yb/Er concentration.

3.4. The ET in Yb^{3+}/Er^{3+} doped tellurite glasses

The ET efficiency from Yb^{3+} to Er^{3+} was evaluated by using the expression [32]

$$n = 1 - \frac{\tau_{Yb-Er}}{\tau_{Yb}}, \tag{5}$$

where τ_{Yb-Er} and τ_{Yb} are the fluorescence lifetimes of the $^2F_{5/2}$ level of codoped Yb^{3+}–Er^{3+} and Yb^{3+} doped glasses. The ET efficiency increases from 36% to 66% by increasing the Er^{3+} concentration and from 56% to 69% by increasing the Yb ions, see figure 10. This last value is in agreement with other reports published recently [33]. The obtained results show that the major changes in ET efficiency occur by increasing the Er concentration (acceptors). One possible explanation for this phenomenon is as follows. Because the absorption cross section of Yb^{3+} ($^4F_{7/2} \rightarrow {}^4F_{5/2}$) is much larger than that of Er^{3+} ($^4I_{15/2} \rightarrow {}^4I_{11/2}$), mostly all of the absorption energy is taken for donors (Yb). Thus, there are many more free donors than acceptors (Er) to make the ET. But with the increment in Er^{3+} concentration, the probability of Er^{3+} absorbing the energy from Yb^{3+} becomes higher and consequently the ET efficiency is increased. The increment in Yb^{3+} concentration increases the probability of forming Yb–Er pairs enhancing the ET, but at the same time the number of acceptors will be reduced explaining the slow increment in ET, see figure 10.

4. Conclusions

Spectroscopic properties of Er^{3+}/Yb^{3+} codoped $70TeO_2$–$20ZnO$–$5Li_2O$–$5La_2O_3$ glass as a function of Er^{3+} and Yb^{3+} concentrations were studied. It was demonstrated that the ECS, the FWHM and the QE of the characteristic 1.53 μm signal can be improved by properly choosing the concentration of both Yb/Er ions. A large concentration of Yb ions improves the signal emitted, partly because it helps in reducing quenching of Er and partly because ET was enhanced. The large QE and stimulated ECS of this signal suggest that this glass composition has strong possibilities of being used in lasers and amplifiers design at the eye safe emission. The increment in Yb ions also strongly increases the upconverted signal. Although such an emission is deleterious to the NIR signal, the strong signal visible to the naked eye open new possibilities of being used in the design of visible laser emission, displays and solid state lighting to mention a few.

Acknowledgments

This work was partly supported by CONACyT, México, through grant 43168F. H Desirena gratefully acknowledges the scholarship for PhD studies provided by CONACyT.

References

[1] Mori A, Ohishi Y and Sudo S 1997 *Electron. Lett.* **33** 863
[2] Ohishi Y, Mori A, Yamada M, Ono H, Nishida Y and Oikawa K 1998 *Opt. Lett.* **23** 274
[3] Vetrone F, Boyer J C, Capobianco J A, Speghini A and Bettinelli M 2002 *Appl. Phys. Lett.* **80** 1752
[4] Chung W J, Jha A, Shen S and Joshi P 2004 *Phil. Mag.* **84** 1197
[5] Kumar G A, De la Rosa E and Desirena H 2006 *Opt. Commun.* **260** 601
[6] El-Mallawany R, Patra A, Friend C S, Kapoor R and Prasad P N 2004 *Opt. Mater.* **12** 34
[7] Lin H, Jiang S, Wu J, Song F, Peyghambarian N and Pun E Y B 2003 *J. Phys. D: Appl. Phys.* **36** 812
[8] Lin H, Meredith G, Jiang S, Peng X, Luo T, Peyghambarian N and Pun E Y B 2003 *J. Appl. Phys.* **93** 186
[9] Dai S, Wu J, Zhang J, Wang G and Jiang Z 2005 *Spectrochim. Acta* A **62** 431
[10] Rolli R, Mongtagna M, Chaussedent S, Monteil A, Tikhomirov V K and Ferrari M 2003 *Opt. Mater.* **21** 743
[11] Zhao S, Wang X, Xu S and Hu L 2005 *Chalcogen. Lett.* **2** 97
[12] . Shi-Xun D, Jun-Jie Z, Shun-Guang L, Shi-Qing X, Guo-Nian W, Jian-Hu Y and Li-Li H 2004 *Chin. Phys.* **13** 2162
[13] Xu S, Wang G, Dai S, Zhang J, Hu L and Jiang Z 2004 *J. Solid State. Chem.* **177** 3127
[14] Gao Y, Qiu-Hua Nie, Tie-Feng Xu and Shen X 2005 *Spectrochim. Acta* A **61** 1259
[15] Hu Y, Jiang S, Sorbello G, Luo T, Ding Y, Hwang B C, Kim J H, Seo H J and Peyghambarian N 2001 *Proc. SPIE* **4282** 57
[16] Byun J, Kim B, Hong K, Jung H, Lee S, Ryoo K, Izyneev A and Kravchenko V B 1994 *Japan. J. Appl. Phys.* **33** 4907
[17] Hayden J, Hayden Y and Campbell J 1990 *Proc. SPIE* **1277** 121
[18] Minami T and Mackenzie J 1977 *J. Am. Ceram. Soc.* **60** 232
[19] Wang J S, Vogel E M and Snitzer E 1994 *Opt. Mater.* **3** 187
[20] Desirena H, Shulzgen A, Shabet S, De la Rosa E and Peyghambarian N submitted
[21] Judd B R 1962 *Phys. Rev.* **127** 750
[22] Ofelt G S 1962 *J. Chem. Phys.* **37** 511
[23] Shen X, Nei Q, Xu T and Gao Y 2005 *Spectrochim. Acta* A **61** 2827
[24] Cho D H, Choi Y G and Kim K H 2001 *ETRI J.* **23** 151
[25] McCumber D E 1964 *Phys. Rev.* A **134** A299
[26] Miniscalco W J and Quimby R S 1991 *Opt. Lett.* **16** 258
[27] Barnes W L, Laming R I, Tarbox E J and Morkel P R 1991 *IEEE J. Quantum Electron.* **27** 1004
[28] Bor-Chyuan H, Jiang S, Luo T, Watson J, Sorbello G and Peyghambarian N 2000 *J. Opt. Soc. Am.* B **17** 833
[29] Li L *et al* 2004 *Appl. Phys. Lett.* **85** 2721
[30] Shen S, Naftaly M and Jha A 2002 *Opt. Commun.* **205** 101
[31] Sumida D S and Fan T Y 1994 *Opt. Lett.* **19** 1343
[32] Zhang L, Hu H, Qi C and Lin F 2001 *Opt. Mater.* **17** 371
[33] Zhang Q Y, Feng Z M, Yang Z M and Jiang Z H 2006 *J. Quantum. Spectrosc. Radiat. Trans.* **98** 167

AQ4

QUERIES

Page 1
AQ1
Please be aware that the color figures in this article will only appear in colour in the web version. If you require colour in the printed journal and have not previously arranged it, Please contact the Production Editor now.

Page 1
AQ2
Please clarify if edits to the sentence 'A broadband larger than...' retain the intended meaning.

Page 2
AQ3
Please clarify if edits to the sentence 'The addition of Na_2O improves...' retain the intended meaning.

Page 7
AQ4
Please provide complete details for 20.

Reference linking to the original articles

References with a volume and page number in blue have a clickable link to the original article created from data deposited by its publisher at CrossRef. Any anomalously unlinked references should be checked for accuracy. Purple is used for links to e-prints at arXiv.